



DYNAMIC ANALYSIS OF AN OFFICE BUILDING FOUNDED OVER A BURIED STREAM DEPOSIT OF LIQUEFIABLE SOILS IN CHRISTCHURCH, NZ

R. Luque ⁽¹⁾, J.D. Bray ⁽²⁾

⁽¹⁾ PhD Candidate, Department of Civil and Environmental Engineering, University of California, Berkeley, USA, roberto.luque@berkeley.edu

⁽²⁾ Professor, Department of Civil and Environmental Engineering, University of California, Berkeley, USA, jonbray@berkeley.edu

Abstract

The New Zealand Canterbury Earthquake Sequence had several large earthquakes that produced different levels of liquefaction-induced ground failure and building damage. As a result, this earthquake sequence and the observations of seismic performance during it provide a unique data set for evaluating state-of-the-art design procedures. This paper focuses on the dynamic soil-structure interaction (SSI) analysis of a shallow founded building that suffered liquefaction-induced differential settlement in the Central Business District of Christchurch. The CTUC building was a 6-story reinforced concrete frame structure, with individual footings tied together by grade beams in both directions, which was demolished due to earthquake damage. Part of the building was founded over a buried stream channel filled with liquefiable silty sand. Nonlinear effective stress fully coupled SSI analyses were performed using FLAC-2D with the PM4Sand constitutive model calibrated with field and lab data. The results show good agreement between observed and calculated responses of the ground and the structure during the key events.

Keywords: Dynamic Analysis, Performance Based Earthquake Engineering, Shallow Foundation, Soil Liquefaction, Soil-Structure Interaction



1. Introduction

The estimation of liquefaction-induced settlement of structures is based largely on empirical procedures to estimate post-liquefaction, one-dimensional (1D) consolidation settlements in the free-field. These 1D volumetric-induced settlement procedures neglect the important effects of the presence of a structure [1]. Recent research [2,3] has found that seismically induced building movements were often controlled primarily by shear-induced ground deformations as a result of soil-structure interaction (SSI)-induced ratcheting and bearing capacity-type movements as well as volumetric ground deformations resulting from localized partial drainage, sedimentation, and post-liquefaction reconsolidation. In addition, the removal of materials beneath a structure due to the formation of sediment ejecta (when it occurs) can have a dominant effect on building performance. The previously mentioned 1D empirical procedures can only capture the settlements related to volumetric strain (i.e., primarily post-liquefaction reconsolidation). Analytical procedures that can capture shear-induced ground deformations are thus required to evaluate liquefaction-induced building settlement.

The results of the numerical analysis of a building that suffered different levels of liquefaction-induced settlement damage in several events during the 2010-2011 Canterbury Earthquake Sequence (CES) are presented in this paper to advance the profession's understanding of liquefaction-induced building settlement. The dynamic SSI analyses were performed using the program FLAC 2D [4] and the user-defined model PM4Sand-Version 3 [5]. The calibration of the model was performed by capturing the likely field Cyclic Resistance Ratio (CRR) vs. Number of Load Cycles (N_{cycles}) relationships resulting from a widely accepted liquefaction triggering procedure. The structure and the underlying soil were modelled, and the calculated building displacements were compared to the observed displacements after three key earthquakes to investigate this phenomenon and to develop recommendations for performing dynamic SSI analyses to estimate liquefaction-induced building movements.

2. Canterbury Earthquake Sequence and Input Ground Motions

The CES included seven events with $M_w \geq 5.5$, three of which had $M_w \geq 6.0$. Ground shaking was recorded at four strong motion stations within the Central Business District (CBD). The 22 FEB 11 Christchurch M_w 6.2 earthquake produced the most intense ground shaking in the CBD, because the source-to-site distances (R) were only 3-6 km. Its peak ground acceleration (PGA) values were twice those recorded during the larger, but more distant ($R = 18-20$ km) 4 SEP 10 Darfield M_w 7.1 event. The PGAs recorded in the CBD during the Darfield event are similar to those recorded during the 13 JUN 11 M_w 6.0 and 23 DEC 11 M_w 5.9 events. The PGA values of the dozens of other earthquakes events are lower than those recorded during these events. This paper focuses on the response during three events: the 4 Sep 2010 M_w 7.1 Darfield event, 22 Feb 2011 M_w 6.2 Christchurch event, and 13JUN11 M_w 6.0 event.

The CTUC Building is located about 1 km to the SE of the REHS station, about 1.1 km NW of the CCCC station, about 1.4 km NE of the CHHC station, and about 1.8 km E of the CBGS station. Recorded geo-mean PGAs at these strong motion stations are provided in Table 1, together with the median PGAs at the CTUC site used for simplified liquefaction evaluation, which were estimated using Bradley & Hughes [6]. There are no outcropping "rock" site recordings to use directly in dynamic SSI analysis. Moreover, the depth to bedrock is not known at these deep soil sites, which are not well characterized below the Riccarton Gravel layer. Thus, recorded ground motions at dense (non-liquefiable) sites in the deep Canterbury basin were used to deconvolved "within" motions in the CBD for the top of the stiff Riccarton Gravel layer, which is at depth of about 24 m at this site. These deconvolved Riccarton Gravel motions were assigned at the base of the numerical model as input motions. The input ground motions were obtained through a SHAKE deconvolution process of recorded ground motions to the Riccarton Gravel as described in [7] and then scaled based on New Zealand-specific ground motion prediction equation (GMPE) [8] to account for the differences in source-to-site distance (R_{rup}) and shear wave velocity in the upper 30 meters (V_{s30}) between the station where the deconvolution was performed and the CTUC building. The uncertainty in the characteristics of the input motions is one of the key limitations of this and other studies of the Christchurch case histories.



Table 1 - Recorded geometric mean Peak Ground Accelerations (PGA) at the four Strong Ground Motion Stations near the CTUC building and median PGA for CTUC based on Bradley & Hughes (B&H) [6]

EARTHQUAKE	STRONG GROUND MOTION STATION				CTUC B&H [6] (g)
	CBGS (g)	CHHC (g)	REHS (g)	CCCC (g)	
DARFIELD	0.17	0.18	0.25	0.21	0.22
CHRISTCHURCH	0.48	0.35	0.51	0.42	0.45
13 JUN 2011	0.19	0.20	0.29	-	0.24

Figure 1 shows, for the three events, the input “within” NS component acceleration–time histories at the top of the stiff Riccarton Gravel layer, their respective response spectra and Husid plots as well as other important ground motion parameters, such as peak ground acceleration (PGA), significant duration (D_{5-95}), arias intensity (I_a), mean period (T_m) and shaking intensity rate (SIR). The motions shown in Figure 1 correspond to the deconvolved motion from the recorded ground motion at the RHSC station. This figure shows the difference in the characteristics of the ground motion in terms of the intensity, duration, and frequency content. The Christchurch earthquake is an intense, intermediate-frequency, short-duration motion compared to the larger magnitude, larger source-to-site distance Darfield record that shows a less intense (half the amplitude), longer duration motion. The 13JUN11 motion has intermediate intensity between the Darfield and Christchurch motions and similar duration to the Christchurch motion.

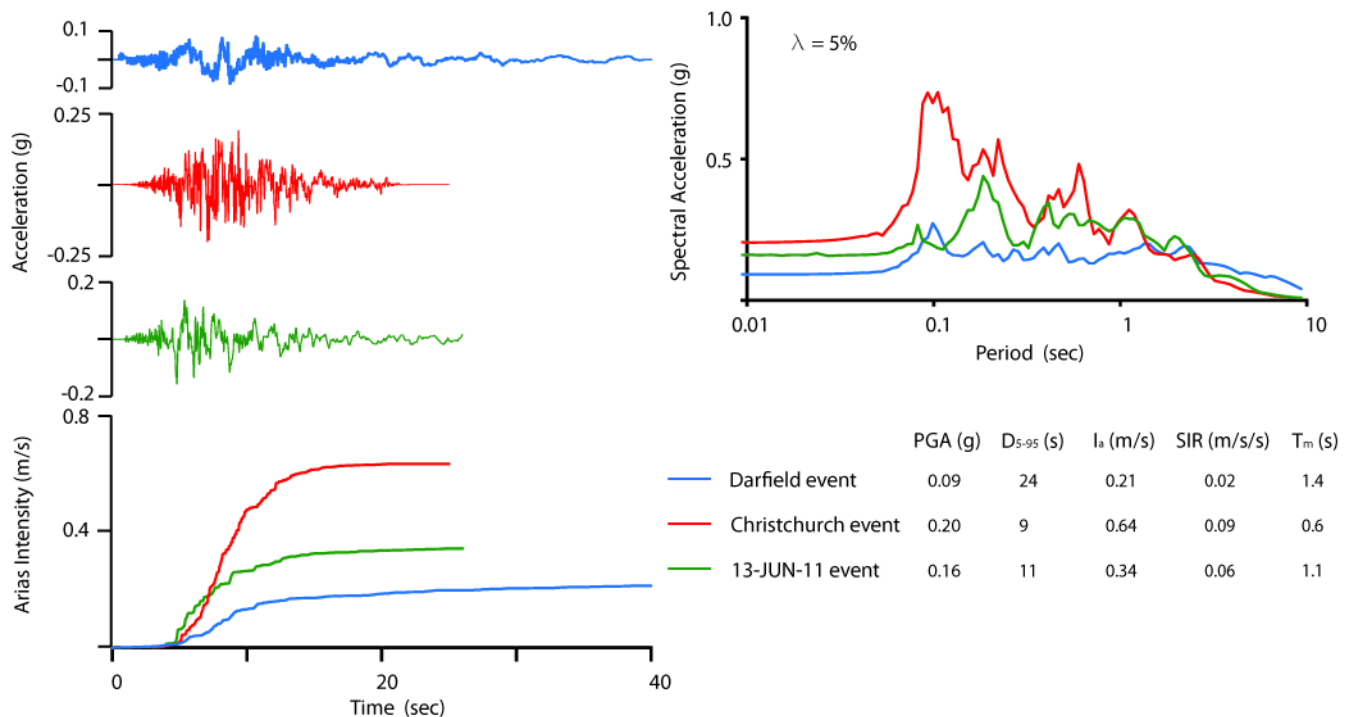


Fig. 1 Deconvolved “within” Riccarton Gravel (from RHSC station) input ground motions for NS component for the three main events, their 5%-damped acceleration response spectra and Husid plots



3. Site Description and Performance Observations

3.1. Building Description

The CTUC office building (S43.5286 E172.6425) was a six-story, reinforced concrete (RC) frame structure supported on individual footings connected with tie beams. Fig. 2 (a) shows the plan view of the foundation of the building together with the two adjacent buildings and the locations and depth of the cone penetration tests (CPTs). Fig. 2 (b) shows the eastern structural frame oriented in the NS direction. The building is 21 m high, 25 m long in the NS direction and 20 m wide in the EW direction [9]. The foundation system consists generally of 2.44-m square footings with a depth of 0.46 or 0.6 m, which support 0.5-m wide square RC columns. The exception to this type of foundation is: (1) a large 9-m square footing where two columns, the elevator, and stair core are founded, which is located on the west side of the building, (2) a 1.3-m wide by 15.44-m long by 0.9-m deep footing oriented in the EW direction and located to the north of the building, which is used as the foundation of a RC block wall, and (3) two 4.88 m by 0.91 m footings with a depth of 0.46 m, each one supporting one of the southern RC columns (0.45 by 1.5 m section) of the building, with their longer side oriented in the EW direction. The two structural frames oriented in the NS direction are connected in their foundation with 0.3 m by 0.38 m tie beams in the EW direction. In the NS direction tie beams of the same dimension connect the three southern spans whereas tie beams 0.61 m by 1.22 m connect the two northern spans. The embedment depth of the footings is 1.2-1.3 m. The spacing between columns is 4.9 m to 5.2 m in the NS direction and 9.15 m in the EW direction.

The columns of the building have a square section with a width of 0.5-m from ground level to the third floor, where they transition to 0.45-m wide square columns to the 5th story. The columns are connected on each floor with 0.4 m by 0.6 m beams in the EW direction. In the NS direction, only the eastern frame is connected through beams of the same size. The floor consists of 0.075-m thick uni-span precast concrete floor with 0.075-m thick RC topping. The top floor (between stories 5 and 6) is a composition of four EW oriented steel frames connected in the NS direction with steel beams. Footing pressures, including dead load and 20% of the live load, were estimated to be in the order of 190–250 kPa.

3.2. Soil Conditions

Subsurface conditions at the site have been characterized using six CPTs, which locations are shown in Fig. 2 (a) and one borehole near CPT Z4-5. Fig. 3, from [9], shows the profile A-A' depicted in Fig. 2 (a). This figure shows the general subsurface conditions between depth of 0 and 20 m near the eastern side of the building. The groundwater depth was estimated to be 2.5 m for the Darfield and Christchurch events, and 2.0 m for the 13JUN11 event based on the T&T groundwater models [10]. The soil stratigraphy consists of a shallow SM/ML layer present along the entire site between the ground surface and 2.5 m depth, with the exception of the south side where this layer extends to 5 m depth. This layer is composed of silty sand and sandy silt (SM/ML) with tip resistance, q_t , generally less than 5 MPa ($D_R \approx 35 - 45\%$) and normalized soil behavior type indices (I_c) generally between 2.0 and 2.5, which makes it likely to liquefy under strong ground shaking when present below the water table. Between this layer and 7.5-9 m depth, a dense gravelly sand is found with q_t values between 20-30 MPa ($D_R \approx 80-90\%$). Then, a medium dense sand and silty sand with q_t values between 10-20 MPa ($D_R \approx 60-70\%$) and I_c values generally between 1.5 and 2.0 is found to a depth of 16-17 m. Within this layer, thin layers of silts and clayey soil layers, with I_c values between 2.6 – 3.2, of variable thickness are found throughout the site. Towards the south, CPT Z4-5 presents several of these clayey layers closely spaced, with average undrained shear strength (s_u) of 150 kPa. From 16-17 m to 21 m depth a dense sand soil layer with q_t values between 25 - 30 MPa ($D_R \approx 80-90\%$) and I_c values between 1.5 and 2 is found. Finally, from 21 m to 24 m depth, an over-consolidated silt-clay layer with I_c values between 2.6 to 3.6 and undrained shear strength of 100-200 kPa overlies the dense Riccarton Gravel unit. In Fig. 3, the red and orange shaded zones correspond to soils with factor of safety against liquefaction (FS_L) lower than unity for the silty soil and the medium dense sand respectively for the Christchurch event using the Robertson & Wride [11] liquefaction evaluation procedure.

Advanced laboratory testing was performed by Markham [12] on soil samples retrieved with the Dames & Moore hydraulic fixed-piston sampler. The density of the material tested (mostly the SM/ML loose soil in CPT Z4-5) was sufficiently low (i.e., $q_{c1n} < 60$) that it is believed that the retrieved soil samples were densified during the sampling process. Denser materials ($q_{c1n} > 60$), such as the medium dense SP/SM material between depth of 10 and 15 m in CPT Z4-5, were retrieved satisfactorily (i.e., without evidence of disturbance) as noted by [12]. Only one sample was retrieved from this unit, so that no liquefaction triggering curve could be obtained. Taylor [13] also performed laboratory testing near this site but all the retrieved samples corresponded to denser soils than the shallow loose SM/ML material that is of special interest in evaluating the seismic performance of this building.

3.3. Seismic Performance Observations

Zupan [9] discusses extensively the performance observations of the CTUC building after several earthquakes. Damage to the CTUC building was negligible during the Darfield and 13JUN11 events, but severe liquefaction in the foundation soils during the Christchurch event induced total and differential settlements, leading to structural distortions and cracking. Fig. 2 (a) shows measured differential settlements in each column relative to the adjacent building to the north which did not appear to settle relative to the surrounding ground. Focusing on the eastern frame, it is apparent that the SE column settled significantly more than the other columns. The differential settlement led to angular distortions of 1/50 in the southern span. In the SE corner was also observed ground ejecta which contributed to the differential settlement. Zupan [9] performed bearing capacity calculations in the SE corner of the building considering the residual undrained strength of the liquefiable sand and found FS below unity. Table 2 summarizes the settlements that occurred in the NE and SE corners of the CTUC building during several CES events. The settlements in Table 2 are categorized by type of settlement (i.e. soil ejecta settlement, volumetric settlement, and shear-induced settlement).

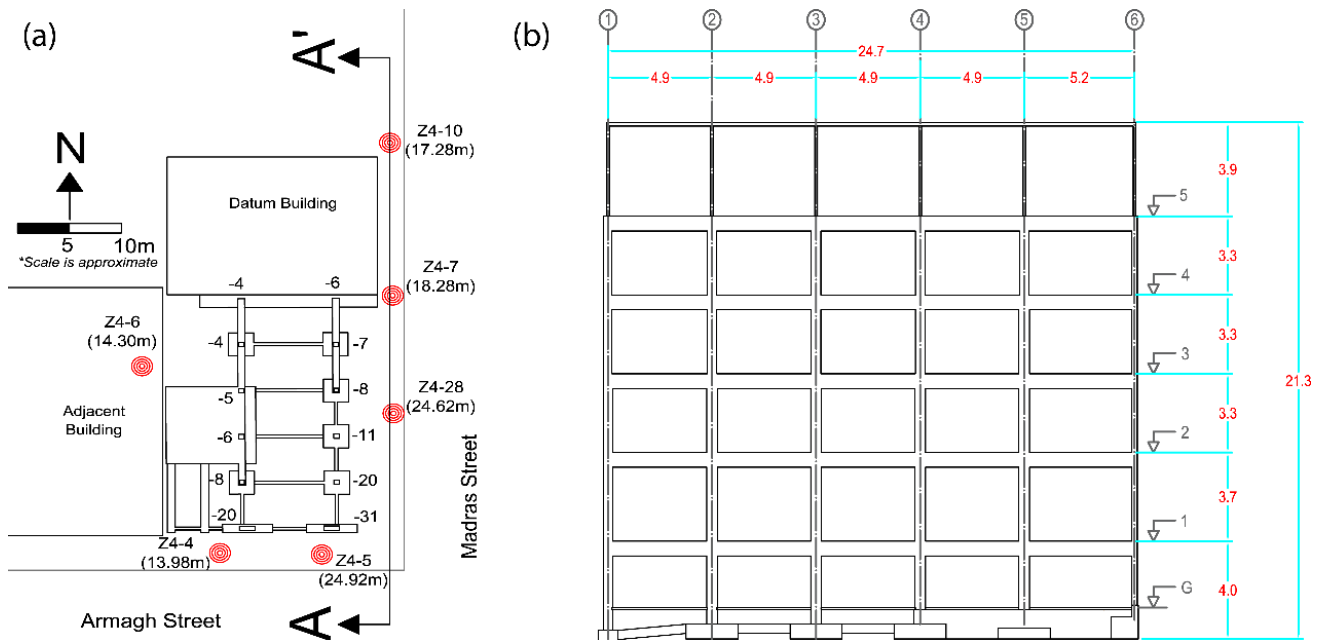


Fig. 2 – (a) CTUC building site with its foundation system, CPT locations, footing settlements (cm) and (b) structural frame corresponding to the NS oriented eastern frame (from [9]).

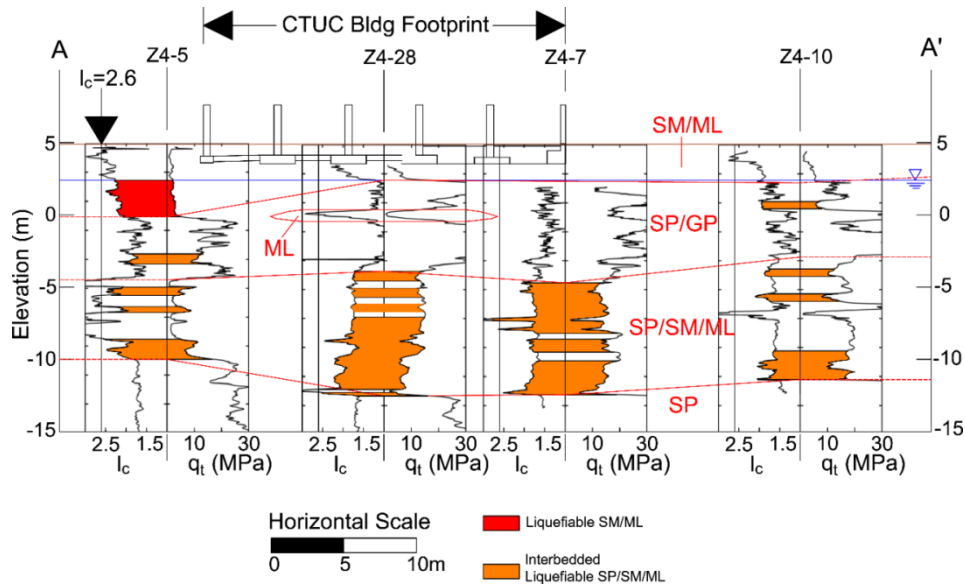


Fig. 3 - Subsurface conditions at the CTUC building site showing zones of materials with $FS_1 < 1.0$ based on the Robertson & Wride [11] procedure using median PGA from [6] for the Christchurch event (from [9]).

Differential punching settlements were measured to be 6 cm and 31 cm in the NE and SE corners, respectively. Ground ejecta were only observed in the Christchurch event in SE corner of the building and values of 5-15 cm were estimated to be caused by soil ejecta based on observations. Volumetric-induced settlement were estimated using [14] procedure with FS_1 obtained from [11]. However, as noted by [9], simplified procedures tend to overestimate settlements compared to observations, especially for the weaker events (Darfield and 13 JUN 11 events), and they slightly underestimate settlements for the Christchurch event. Thus, for the two weaker events, the estimated volumetric deformations were reduced (i.e., by 30-40%). Total liquefaction-induced settlements of about 15-30 cm and 50-75 cm were estimated for the NE and SE corners of the CTUC building, respectively.

4. Calibration of the constitutive model

The PM4Sand Version 3 [5] constitutive model was used to model sandy soils. The model was calibrated against the simplified liquefaction triggering procedure. There was an absence of a reliable laboratory-based cyclic resistance data because of sampling disturbance in the loose SM/ML unit ($q_{c1n} < 35$) that was directly beneath the southern side of the CTUC building. For clayey soils, the Mohr-Coulomb model with hysteretic damping was used. PM4Sand model parameters were developed using best-estimated median values of unit weights (γ), relative densities (D_R) and shear wave velocities (V_S). These parameters were obtained through correlations with the CPT, such as Robertson [15] for unit weight; Idriss and Boulanger [16] – herein called I&B-08-, Kulhawy and Mayne [17] and Jamiolkowski [18] with weights of 0.4, 0.3, and 0.3, respectively, for D_R ; and the McGann [19] Christchurch-specific correlation between CPT data and V_S , which then was used to obtain the normalized shear modulus (G_o). With these parameters and the confining pressure of the different units, element tests were modeled in FLAC 2D [4] and the contraction parameter (h_{po}) was varied to obtain the CRR at 15 cycles of loading obtained from the Boulanger and Idriss [20], herein called B&I-16, simplified liquefaction procedure. The 50% probability of liquefaction curve was used for this calibration, because a median estimate was desired for the back-analysis (instead of a conservative design estimate using $P_L = 15\%$). Table 3 summarizes the average values of unit weight, relative density, normalized shear modulus and the calibrated values of the contraction parameter for each layer. Other secondary model parameters, such as critical state line parameters ($Q = 8.0$ and $R = 1.0$), critical state friction angle ($\phi_{cs} = 35$ degrees), bounding surface parameter ($n_b = 1.4$ degrees), and e_{max} and e_{min} , were obtained from available laboratory testing of the Christchurch soils [12, 13].



Table 2 – Settlement of the CTUC building

Type of Settlement	NE corner		SE corner	
	Measured (cm)	Estimated (cm)	Measured (cm)	Estimated (cm)
Liquefaction-Induced Punching Settlement ¹	6		31	
Shear-Induced Settlement ²		6		17 – 22
Ground Ejecta Settlement ³		0		0
		0		5 – 10
		0		0
		0		5 – 10
Volumetric-Induced Settlement ⁴		0 – 1		0 – 2
		10 – 17		10 – 20
		0 – 2		0 – 2
		10 – 20		10 – 24
Total Liquefaction-Induced Settlement		16 – 26		32 – 56

Values for each event and the total values are presented as follows: Blue is for the Darfield (4 Sep 2010) event, Red is for the Christchurch (22 Feb 2011) event, Green is for the 13 JUN 2011 event, and Black is the total for the three events.

¹ Settlement taken relative to the adjacent building to the North, which did not appear to settle relative to the surrounding ground. This settlement includes shear-induced settlement and the ground ejecta settlement; ground ejecta was only observed at the two columns in the SE corner.

² Shear-induced settlement was estimated by subtracting the estimated ground ejecta settlement from the measured liquefaction-induced punching settlement, with a slight adjustment due to the minor difference in the estimated volumetric-induced settlement across the building footprint.

³ Ground ejecta settlements were estimated based on the amount of ejecta that was observed at the ground surface.

⁴ Volumetric-induced settlement of ground was estimated using the Zhang et al. (2002) [13] procedure based on [9].

Table 3 – Primary parameters and properties used for the PM4 Sand model for cohesionless soils.

Soil Layer	γ (kN/m ³)	D_R (%)	G_o	h_{po}
Loose silty sand /sandy silt [SM/ML]	16.6	40	400	1.2
Dense gravelly sand/sandy gravel [SP/GP]	19.7	85	1500	3.0
Medium dense sand/silty sand [SP/SM/ML]	19.3	65	900	0.3
Dense silty sand/sand [SP/SM]	20.3	85	2000	7.0

Fig. 4 shows the calibration for the loose SM/ML shallow layer shown in Fig. 3. The CRR- N_{cycles} curve from the element test simulations is shown in blue dots together to the power function fitted to it. The slope of the curve in the numerical simulation is controlled by the bounding surface [5], which is defined by the parameter n_b and which was obtained from the results of isotropically consolidated drained triaxial compression (CIDC) tests performed by [13]. In the case presented in Fig. 4, the slope of the CRR- N_{cycles} curve that resulted from the numerical simulation is in good agreement with the magnitude scaling factor (MSF) relationship implied by the I&B 08 method. However, other soil units, may present slopes that are in more agreement with the updated density-dependent MSF relationship implied by the B&I-16 MSF relationship.

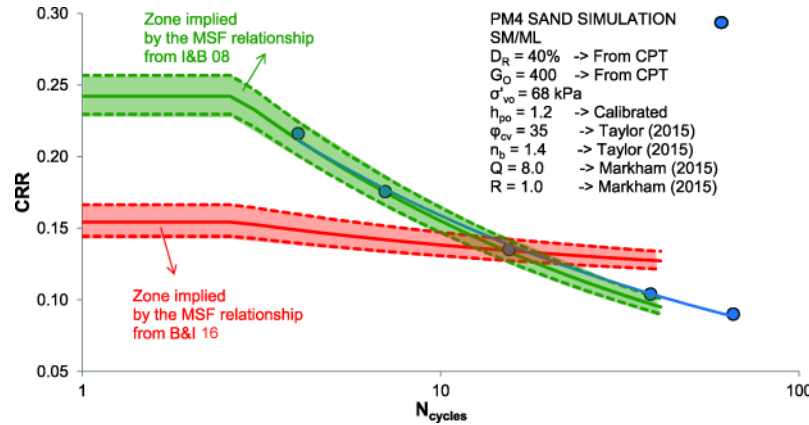


Fig. 4 – Calibration of the constitutive model to the triggering curves implied by the MSF relationship from Boulanger and Idriss (2008) for the loose shallow silty sand/sandy silt (SM/ML) layer

5. Free-Field Ground Response

The soil profile considering the horizontal variation in the stratigraphy identified by the CPTs was modeled without the presence of the building to evaluate the free-field response of the site. The responses in terms of horizontal acceleration, pore pressure ratio, and shear strain were computed at several locations and compared to the results of the factor of safety against liquefaction (FS_1) from the B&I-16 simplified liquefaction procedure. Additionally, the computed 5%-damped acceleration response spectrum at the surface was compared to the response spectra recorded at the four strong ground motion stations in the CBD.

Fig. 5 (a) and (b) shows the calculated responses at the SE and NE corners of the CTUC building, which coincides with the location of CPTs Z4-5 and Z4-7, respectively. These responses are compared to the factor of safety for liquefaction triggering (FS_1) using the B&I-16 procedure for the three events analyzed. The FLAC analyses calculate zones of high pore pressures ratio and shear strain in zones where the simplified procedure gives $FS_1 < 1$. The differing levels of calculated shear strain highlight the differences in the soil response during each of these events. The Christchurch event produces shear strains in the order of 1 - 1.5%, the 13 JUN 11 event $< 0.7\%$, and the Darfield event $< 0.2\%$. The simplified liquefaction evaluation suggests the Darfield event should be slightly more damaging (lower FS_1) than the 13 JUN 11 event. However, more liquefaction-induced damage in the CBD was observed for the 13-JUN-11 event, which is also supported by the analytical results in terms of pore pressure ratio and shear strains. The effect of the response of shallow layers due to high pore water pressure generation on the calculated seismic site response is an important issue with dynamic analyses of soil profiles under a vertically propagating horizontal shear wave excitation. Lastly, relatively high values of pore pressure ratios (i.e., > 0.5) do not necessarily translate into high shear strains as shown for the 13 JUN 11 event.

Fig. 6 shows the 5%-damped acceleration response spectra at the surface from the analyses for the Christchurch, Darfield, and 13 JUN 11 earthquakes with the NS component response spectra from the recorded motions in the four CBD strong ground motion stations in the background. For the 13JUN11 event, the CCCC station did not record the motion, thus only the response spectra for the three remaining stations are shown in Fig. 6 (c). The results show good agreement between calculated response spectra and recorded spectra for the Christchurch and Darfield events. The 13 JUN 11 event analyses give a slightly stronger response than the recorded response in the CBD. This leads to greater liquefaction being calculated for this event relative to the Darfield event.

Fig. 6 also shows the difference in the site response from the north and south sides of the building. The absence of the loose liquefiable layer at the north side (near CPT Z4-7) results in higher frequency content motions calculated at the ground surface with peaks in the response spectra at periods of around 0.2 seconds. Conversely, the south side results in spectra with a wider zone of peaks between 0.5 and 1 seconds. In general, the south side (near CPT Z4-5) has a higher Peak Ground Acceleration (PGA). For periods greater than 1 – 2 seconds the spectral ordinates are similar for both the north and south sides of the CTUC building.

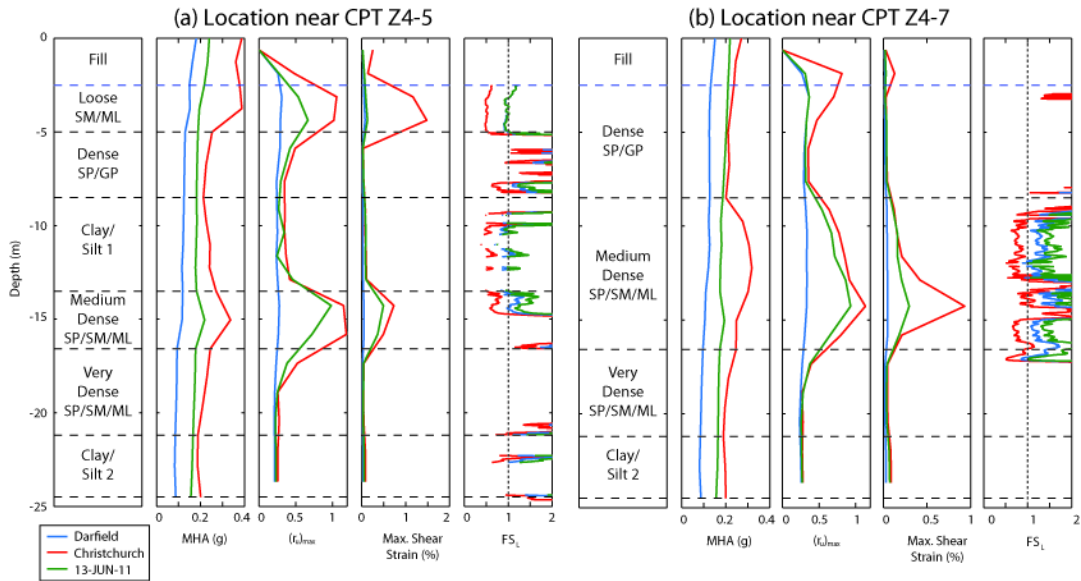


Fig. 5 – Results of the CTUC site in a free-field condition using the motions deconvolved from the RHSC station for (a) CPT Z4-5 and (b) CPT Z4-7

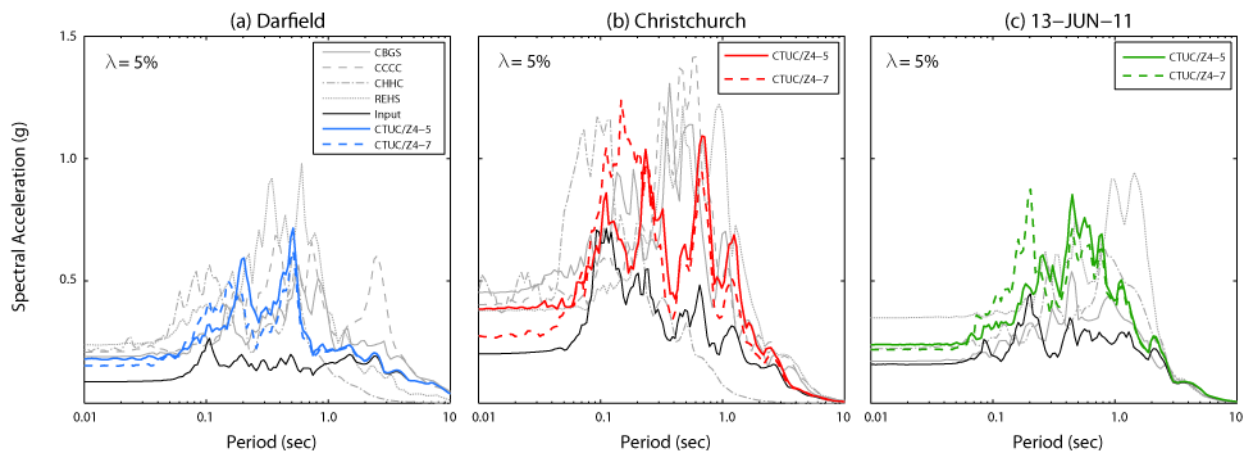


Fig. 6 – 5%-damped acceleration response spectra calculated for the CTUC building at the locations of CPTs Z4-5 and Z4-7 overlying the response spectra of NS component recorded motions at stations in the CBD.

6. Building response

The structural frame oriented in the NS direction located on the east side of the building was modeled. The frame elements were modeled using linear elastic elements. The elasticity young's modulus and unit weight of concrete used for the analyses were 2.35×10^7 kPa and 24 kN/m^3 , respectively. The flexural cracking of the structural elements was considered by applying a factor of 0.35 and 0.7 to the inertia of beams and columns, respectively [20]. Beams oriented in the direction of the analysis were modelled considering the contribution to the stiffness of the floor slab by using an effective width following the recommendations of [20]. The 3D properties of the building were considered by introducing a typical frame spacing of 9.1 m. This spacing is used to scale properties and parameters to account for the effect of the distribution of beams in the EW direction. The vertical loading included in the model was composed of 100% the gravity loading and 20% of live load, which was considered to be 3 kPa per floor. The footings were modelled as structural beam elements attached to the grid. The input motion was a “within” motion applied on a rigid base. Fig. 7 shows the model of the building together with the geotechnical model, the finite element mesh, points “S” and “N”, which are points where the vertical displacement of the corresponding columns was measured during the analyses and the approximate location of the CPTs.

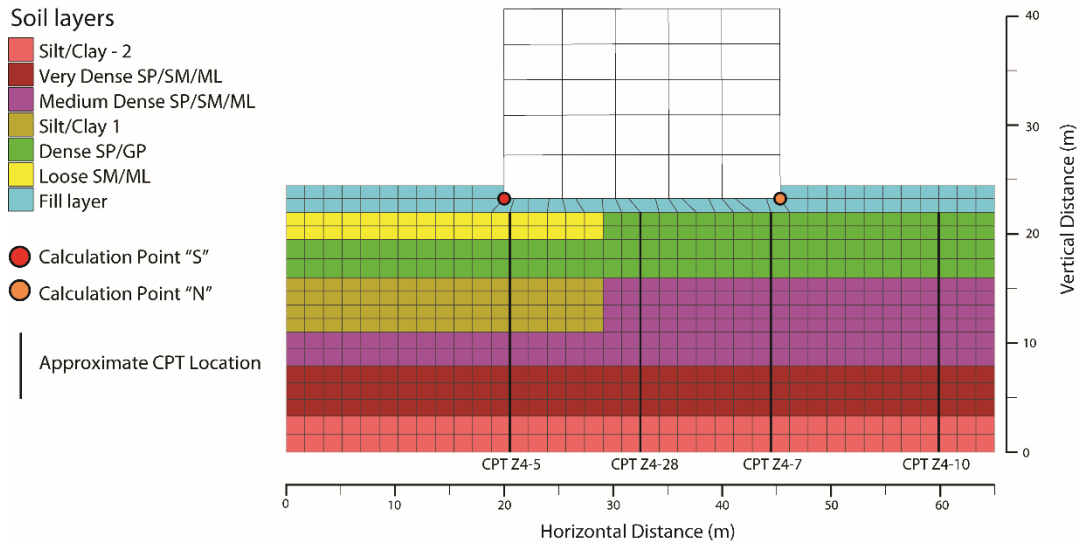


Fig. 7 – Geotechnical and structural model for the CTUC building showing points where important parameters were measured during the analyses.

The vertical displacements at points “S” and “N” are presented in Fig. 8 (a), (b), and (c) for the Christchurch, Darfield, and 13 JUN 11 events, respectively. Fig. 8 (d) shows the post 13-JUN-11 settlement profile along the analyzed section as well as the measured profile. The settlements shown in Fig. 8 (a) – (c) represent the seismic settlement (i.e., during strong shaking), which is mostly shear-induced settlement. Some volumetric-induced settlement that occurs during strong shaking is also included. However, these analyses do not capture the majority of volumetric post-liquefaction re-consolidation settlements that occur after shaking due to dissipation of excess pore water pressure. The analyses also do not include settlement due to the formation of sediment ejecta. Thus, the sum of the presented settlements in Fig. 8 (a)-(c) for the three events is comparable to the estimated shear-induced settlement presented in Table 2 and shown in shaded gray in Fig. 8 (d).

The results show how the different soil conditions under the southern and northern ends of the building affects the seismic performance of the building. There is a shallow loose silty sand layer from a buried stream present only under the southern side of the building. This layer causes significantly more shear-induced ground settlement under the southern side of the building. The sensitivity of the building displacements due to the input ground motion and the characteristics of the loose SM/ML liquefiable layer was evaluated resulting in the range of displacements shown in the red shaded zone shown in Fig. 8 (d). The amount of shear-induced settlement is overestimated slightly in the dynamic SSI analyses. As shown in Fig. 8(d), the range of calculated shear-induced settlement settlements is 22–50 cm and 6–14 cm in the SE and NE corners of the CTUC building, respectively. Estimated values for this mechanism were in the order of 17–22 cm and 6 cm for the SE and NE building corners, respectively. However, the differential settlement across the building footprint, which is most important evaluating seismic performance of the structure, is captured well by the numerical analyses.

The dynamic SSI analyses are also useful in identifying potential failure mechanisms. The CTUC building performance was driven primarily by a bearing capacity-type of failure of the foundations near the SE corner of the building. The SE exterior column is founded on a 4.88 m by 0.91 m spread footing that has loose silty sand/sandy silt just 1.3 m below it. This mechanism leads to excessive shear-induced settlements. There is a concentration of earthquake-induced shear strains calculated within the liquefiable soil just below the SE corner of the building. The large shear strains that develop beneath the southern part of the building foundation, where the soil displaces laterally and upwards, are the primary difference between the responses of the building at its SE and NE corners. In the free-field case (shown in Figure 5), localized shear strain in the order of 1-2% occurs within the shallow liquefiable layer. Under the building foundation, shear strains in the order of 8% are calculated within the same shallow loose silty sand/sandy silt layer.

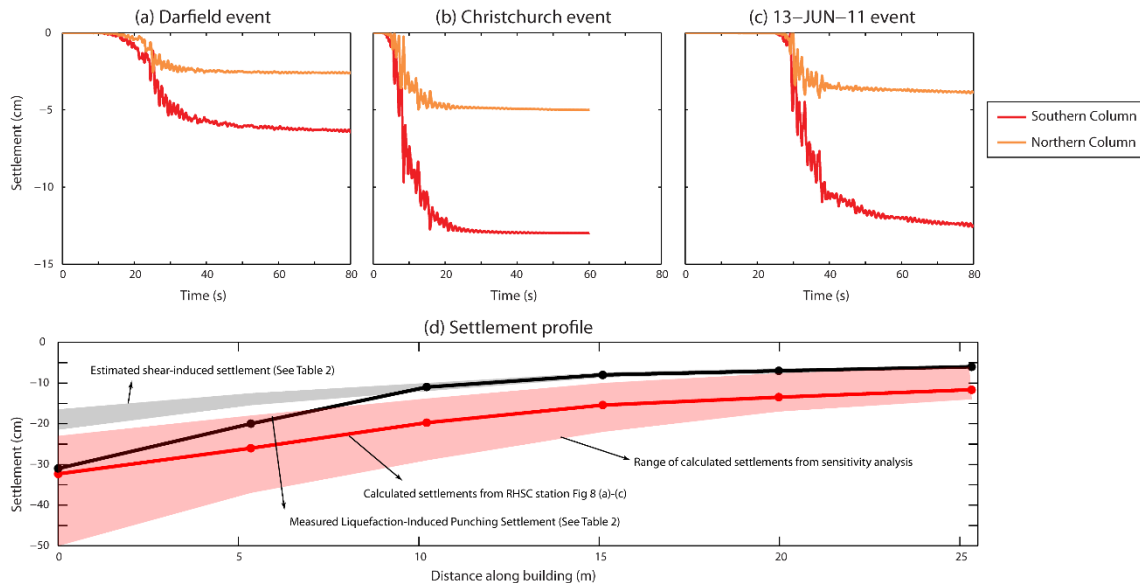


Fig. 8 - Displacement time-histories at the southern column (Point “S”) and at the northern column (Point “N”) for (a) Christchurch, (b) Darfield, and (c) 13JUN11 events, and (d) settlement profile along the building.

7. Conclusions

Soil liquefaction-induced building displacements cannot be estimated directly using simplified empirical procedures that only estimate 1D post-liquefaction reconsolidation (volumetrically induced) settlements, because these procedures do not capture the important shear mechanisms involved in building settlements. Dynamic SSI nonlinear effective stress analysis can capture the critically important liquefaction-induced shear deformations. The dynamic SSI analyses of the CTUC building were able to capture the observed trends in the seismic differential settlement measured in the three primary earthquakes of the Canterbury Earthquake Sequence. However, the analyses require sound characterizations of the site and earthquake shaking. The satisfactory comparison of field observations and analytical results of the CTUC building was only accomplished after calibrating the soil constitutive model such that the response of free-field 1D seismic site response analyses were in general agreement with the results from well-established empirically based simplified liquefaction evaluation procedures. The variation of the soil profile across the CTUC building footprint, which at one end of the building included a shallow loose sand and silty sand deposit from a buried stream channel, produced the observed differential settlement of the building. The analyses also indicated that the observed significant differential settlement was a largely result of a bearing capacity-type of failure in the SE corner of the building. The inability of continuum based soil models to capture the effects of soil ejecta should be recognized as an important limitation for cases wherein this particular mechanism governs performance.

8. Acknowledgements

We wish to acknowledge the National Secretary of Higher Education, Science, Technology and Innovation of Ecuador (SENESCYT) for funding this research. Additional support was provided from the U.S. National Science Foundation (NSF) through CMMI-1332501. Any opinions, findings, and conclusions or recommendations expressed in this material are those of the authors and do not necessarily reflect the views of NSF or SENESCYT. Collaborations with Prof. Misko Cubrinovski and Dr. Merrick Taylor of the University of Canterbury (UC) were invaluable, as well as interactions with UC Berkeley researchers J. Zupan, C. Markham, and C. Beyzaei. Discussions with Prof. Ross Boulanger (UC Davis) and Prof. Katerina Ziotopoulou (Virginia Tech) about the constitutive model were also invaluable.



9. References

- [1] Tokimatsu, K., and Seed, H.B. (1987). "Evaluation of Settlement in Sands Due to Earthquake Shaking." *Journal of Geotechnical Engineering*, 113, 861 – 878.
- [2] Dashti, S., Bray, J.D., Pestana, J.M., Riemer, M.R., and Wilson, D. (2010a). "Mechanisms of seismically-induced settlement of buildings with shallow foundations on liquefiable soil." *J. Geotech. Geoenv. Eng.*, 136(1), 151-164.
- [3] Dashti, S., Bray, J.D. (2013). "Numerical simulation of Building Response on Liquefiable Sand" *Journal of Geotechnical and Geoenvironmental Engineering*, 139(8), 1235-1249.
- [4] Itasca (2009). *Flac – Fast Lagrangian Analysis of Continua*, Version 6.0, Itasca Consulting Group, Inc., Minneapolis, Minnesota.
- [5] Boulanger RW, Ziotopoulou K. PM4Sand (Version 3): A sand plasticity model for earthquake engineering applications. Report no. UCD/CGM-15/01, Center for Geotechnical Modeling, Department of Civil and Environmental Engineering, University of California, Davis, CA; 2015, 108 pp.
- [6] Bradley, B.A., and Hughes, M. (2012). "Conditional Peak Ground Accelerations in the Canterbury Earthquakes for Conventional Liquefaction Assessment." Tech. Report for the Depart. of Building & Housing, 22 pp.
- [7] Markham C., Macedo J., Bray J.D. (2014). "Evaluating Fully Nonlinear Effective Stress Site Response Analyses using Records from the Canterbury Earthquake Sequence". USGS Technical Report.
- [8] Bradley, B.A. (2013). "A New Zealand-Specific Pseudo-spectral Acceleration Ground-Motion Prediction Equation for Active Shallow Crustal Earthquakes Based on Foreign Models." *Bulletin of the Seismological Society of America*. Vol. 103, No. 3, pp. 1801-1822, June 2013.
- [9] Zupan, J. (2014). "Seismic Performance of Buildings Subjected to Soil Liquefaction" Ph.D. dissertation, University of California, Berkeley, Berkeley, CA.
- [10] Canterbury Geotechnical Database (2014). "EQC Event Specific Groundwater Surface Elevations", Map Layer CGD0800 - 09 Jun 2014, retrieved 1 July, 2015 from <https://canterburygeotechnicaldatabase.projectorbit.com/>.
- [11] Robertson, P.K., and Wride, C.E. (1998). "Evaluating cyclic liquefaction potential using the cone penetration test". *Canadian Geotechnical Journal*, Ottawa, 35(3):442-459.
- [12] Markham. C. (2015). "Response of Liquefiable Sites in the Central Business District of Christchurch, New Zealand". Ph.D. Dissertation, University of California, Berkeley, CA.
- [13] Taylor, M. (2015). "The Geotechnical Characterization of Christchurch Sands for Advanced Soil Modelling" Ph.D. Dissertation, University of Canterbury, New Zealand.
- [14] Zhang, G., Robertson, P.K. and Brachman, R.W.I. (2002). "Estimating Liquefaction induced Ground Settlements from CPT for Level Ground". *Canadian Geotechnical Journal*, Ottawa, 39(5):1168-1180.
- [15] Robertson, P.K., (2010). "Soil behavior type from the CPT: an update". 2nd International Symposium on Cone Penetration Testing, CPT'10, Huntington Beach, CA, USA. www.cpt10.com
- [16] Idriss I, Boulanger R. Soil Liquefaction during Earthquakes. Earthquake Engineering Research Institute (EERI), MNO-12; 2008.
- [17] Kulhawy, F.H. and Mayne, P.H. (1990). *Manual on estimating soil properties for foundation design*. Electric Power Research Institute, August, 1990.
- [18] Jamiolkowski, M., LoPresti, D.C.F., and Manassero, M. (2001). "Evaluation of Relative Density and Shear Strength of Sands from Cone Penetration Test and Flat Dilatometer Test." *Soil Behavior and Soft Ground Construction (GSP 119)*, American Society of Civil Engineers, Reston, Virginia, 201 – 238.
- [19] McGann, C., Bradley, B., Taylor, M., Wotherspoon, L., and Cubrinovski, M. (2014). "Development of an empirical correlation for predicting shear wave velocity of Christchurch soils from cone penetration test data." *Soil Dynamics and Earthquake Engineering*, 00(0), 15–27.
- [20] Boulanger, R.W. and Idriss, I.M. (2016). "CPT- Based Liquefaction Triggering Procedures." *Journal of Geotechnical and Geoenvironmental Engineering*, 142(2), 04015065.
- [21] American Concrete Institute (2014). *Building Code Requirements for Structural Concrete (ACI 318-14) and Commentary (ACI 318R-14)*